NOLTR 69-125

SUPERSONIC ABLATION STUDIES WITH TEFLON

6 OCTOBER 1969

NOL

UNITED STATES NAVAL ORDNANCE LABORATORY, WHITE OAK, MARYLAND

NOLTR 69-125

NOLTR 69-125

SUPERSONIC ABLATION STUDIES WITH TEFLON

Prepared by:
E. M. Winkler, M. T. Madden,
R. L. Humphrey and J. A. Koenig

ABSTRACT: An experimental program has been carried out in the Naval Ordnance Laboratory (NOL) 3 Megawatt Arc Tunnel to study the interaction of ablation and a vehicle's aerodynamic characteristics. The test conditions involved stagnation pressures of 20 to 30 atmospheres, temperatures of 4000 to 9000°R and Mach numbers of 2.3 and 3. The test models, made of teflon, were instrumented for pressure, temperature, heat transfer, and skin-friction measurements. Laminar and turbulent boundary-layer data were obtained. The laminar data were compared with the predictions of a numerical procedure known as BLIMP-CMA. Surprisingly close agreement was found between most of the experimental data and predictions. Ablation-induced transition was observed in all laminar runs. In fully turbulent runs cross-hatched striations were observed. Ablation reduced the wall shear stress by about 60 percent for the laminar runs and by 40 percent for the turbulent runs.

U. S. NAVAL ORDNANCE LABORATORY
WHITE OAK, MARYLAND

NOLTR 69-125

6 October 1969

Supersonic Ablation Studies with Teflon

The report summarizes studies of the interaction process between an ablative heat shield and the vehicle aerodynamics. The project was supported by the Independent Exploratory Development Program, Task Number MAT-03L-000-F008-9812, Problem 027, and the Naval Ordnance Systems Command, ORDTASK 351-001/029-1/UF 20-322-502.

The authors wish to thank Dr. E. L. Harris for his continuing interest in the investigations and for many stimulating discussions during the course of the study. The authors also acknowledge the contributions to this program made by Mrs. C. H. Piper and Messrs. M. I. Schlesinger, J. R. Bruno and F. A. Woehr who were responsible for the computation of the nozzle contours, the mechanical design of the nozzles, and the design and instrumenting of the models. The authors also wish to acknowledge Dr. R. M. Kendall and Mr. E. P. Bartlett of the Aerotherm Corporation for their helpful suggestions regarding the use of the BLIMP-CMA computer programs.

GEORGE G. BALL
Captain, USN
Commander

L. H. SCHINDEL
By direction

CONTENTS

ILLUSTRATIONS

TABLES

LIST OF SYMBOLS

A	= cross-sectional area of node
A_s	= original surface area (before ablation)
B	= factor in density law
C_H	= Stanton number
c_f	= skin-friction coefficient
c_p	= heat capacity
E/R	= activation energy
f	= stream function
H_o	= total enthalpy
h	= local enthalpy
$\tilde{K}$	= mass fraction
k	= thermal conductivity
M	= Mach number
m	= reaction order
$\dot{m}_c$	= mass removal rate per unit area of surface material, (e.g. char and its degradation products)
$\dot{m}_g$	= mass removal rate per unit area of gas which enters the boundary layer without phase change at the surface (e.g. pyrolysis gas)
p_o	= supply pressure
p'_o	= Pitot pressure
q	= heat flux per unit area
R	= universal gas constant
T	= temperature
T_o	= supply gas temperature
t	= time

u = velocity in flow direction

v = velocity normal to wall

x = axial distance in flow direction

y = coordinate normal to ablating wall with origin fixed relative to back wall

z = depth, measured from receding surface

α_H = normalizing parameter for boundary-layer coordinate, η, normal to surface

Γ = volume fraction of resin in plastic

δ = nodal thickness

δ^* = boundary-layer displacement thickness

η = non-dimensional wall distance

θ = boundary-layer momentum thickness

ρ = density

ρ_o = original density

ρ_r = final density

τ_w = wall shear stress

Subscripts

A, B, C } identifies components

c = char

e = boundary-layer edge condition

g = gas

i = species or nodal point

k = element

o = total

r = reference

y = location within boundary layer

cond. = conduction

diff. = diffusion

rad in = radiation towards surface

rad out = radiation from surface

Superscript

* = removal from surface in a condensed phase

INTRODUCTION

The use of ablative materials for the thermal protection of re-entering vehicles has not always been entirely successful. Though generally accepted as the means to maintain the substructure temperature at tolerable levels, certain aerodynamic anomalies have been observed that interfered with the proper performance of the vehicle. The anomalous behavior is significant at altitudes below 100,000 feet altitude. The process is not adequately understood, but it is possibly linked with the interaction of ablation and the vehicle's aerodynamics. In addition to the force anomalies, preferential ablation patterns and cross-hatched striations are observed under certain flight conditions that probably have a bearing on the performance of the vehicle. To study the processes, research programs were carried out at NOL which combine experimental investigations in the NOL 3 Megawatt Arc Tunnel and an analytical procedure that allows prediction of the laminar boundary-layer parameters for an ablative surface.

APPROACH

Because of the lack of a proven analytical description of the phenomena involved when the program was initiated in FY 1967, the planned approach was primarily experimental. This was thought to provide data of immediate practical interest as well as to support the development of a theoretical prediction. The program thus endeavored to produce actual flight conditions in the 3 Megawatt Arc Tunnel. For a typical IRBM this required the stagnation conditions shown on Figure 1. Typical values for the stagnation point pressure and enthalpy (for an IRBM with w/C_DA = 700 lbs/ft^2 at 50,000 feet altitude) is 35 atm and 4100 BTU/lb. These conditions can nearly be reached in the NOL arc heater, although we usually operate at somewhat less than 35 atm. Because of the manner the boundary layer develops on blunted bodies, the simulation of flight conditions on a blunted re-entry vehicle can be produced by expanding the gas from a reservoir whose supply conditions are the same as the stagnation point conditions to a free-stream Mach number that equals the local Mach number at the vehicle's station to be studied. This can be a relatively low Mach number (about 3 for a blunted slender cone), in spite of the fact that the flight Mach number is hypersonic. One also has the option to either study the flow external or internal to a model with equal validity of the results. The latter approach is experimentally quite attractive since it allows the easy and ample instrumenting of the model. It was therefore selected. The experiments were designed for testing at Mach numbers of 2.3 and 3 and for providing data on boundary-layer parameters and material responses that will assist the development of theory or at least can be used for empirical correlations of critical parameters. The measured quantities were to include static pressure, Pitot pressure, in-depth wall temperature, surface temperature, local skin friction and total ablation.

EXPERIMENTAL ARRANGEMENT

With the decision to study the flow internal to a model, the experimental set-up became quite simple. It is shown in Figures 2 and 3. The arc heater, described in detail in References 1 and 2, discharges the heated gas into axially symmetric contoured nozzles where it expands to the design Mach number, 2.3 or 3. The flow then enters axially symmetric ducts made of the ablative material. Teflon TFE-7 has been used exclusively during the present test series. The nozzle, as well as the duct contours, were corrected for the boundary-layer growth using available NOL computational procedures, References 3 and 4. The flow then discharges into a diffuser and exhaust system.

The teflon ducts had a nominal I.D. of one inch and a wall thickness of 0.75 inch. They were six inches long. This length was found in prior tests to sustain uniform flow of the design Mach number. At the upstream end the ducts were tightly connected to the water cooled nozzle. At the downstream end the flow discharges as a free jet. A total of eleven ducts were tested. All but one duct were provided with static pressure orifices at $x = 0.25$, 1.25, 2.375, 3.5 and 4.625 inches from the nozzle exit plane. The 4.625 inch station had two pressure orifices, 90 degrees apart to check on the symmetry of the flow. Some ducts were instrumented with surface thermocouples, or had thermocouple plugs (Fig. 4) installed for in-depth temperature measurements. Skin-friction measurements were made during four tests. The balance used is an NOL development described in Reference 5. The balance records continually. Its small time constant and insensitivity to tunnel noise has made the transient measurements possible. The balance is shown in Figure 5 in an exploded view. Pitot pressure measurements were made at the exit of the ducts in all tests, and for one duct a centerline traverse was made to determine the uniformity of flow. The Pitot probes were either water-cooled or uncooled depending on the expected length of exposure to the flow. They were mounted on the quick-injection mechanism described in Reference 1. For tests requiring only a check of the Pitot pressure at the centerline to ascertain the proper running conditions uncooled probes were used because they were simpler to handle. Water-cooled probes, as shown in Figure 6, were used to obtain duct exit traverses. Their use was not entirely satisfactory. The small size of the probes needed for the present test series conflicted with cooling requirements and wall thickness necessary to withstand the aerodynamic and thermal load for an entire traverse. Ablation was determined from contour measurements prior and after the runs. The tunnel supply conditions were computed from the measured pressure, mass flow, and known nozzle throat sizes using the method of Reference 6.

Table I summarizes the tunnel operating conditions and duct instrumentation for all eleven tests. Only tests 1L through 6L were carried out under conditions where the boundary layer was

predicted to be laminar, at leasv for part of the duct. Tests 1T through 5T are a turbulent boundary-layer test series. The latter tests and results are covered in detail in Reference 7. Only some of the results will be included in the present report.

ANALYTICAL PROCEDURES

Two analytical programs have been used in the analysis of the experimental data. These are the Boundary Layer Integral Matrix Procedure and the Charring Material Ablator Program, (BLIMP-CMA), which were acquired from the Aerotherm Corporation, References 8 and 9. These two procedures are fairly versatile and permit calculation of teflon ablation rates, boundary-layer parameters and material responses along axisymmetric or planar surfaces. Quasi-steady or transient solutions can be obtained.

The BLIMP Program incorporates a modified form of the Scala relation for the ablation of teflon, References 10 and 11, which states that the process is rate controlled over the surface temperature range of interest. Scala has assumed that the ablation of teflon is a quasi-steady depolymerization process, according to Reference 12, where the depolymerization of the teflon polymer is considered of first order with respect to the weight of the solid. He also retained the combustion term in the equation, which greatly improved the agreement between predicted and observed ablation rates. Other assumptions which make the program quite general for various applications are that (a) surface reactions and reactions through the boundary layer and discontinuous wall conditions corresponding to a change in material are allowed, (b) the flow is in equilibrium except that certain species may be considered frozen or allowed to react at finite rates, (c) there is an option that allows equal or unequal diffusion and thermal diffusion coefficients, (d) the entropy layer, energy balance, or mass balance concepts can be used. For the present application, the options of a reacting surface, an equilibrium air boundary layer, unequal diffusion coefficients, and a discontinuous wall condition were used. The latter was required because of the nonablating cold wall nozzle upstream of the teflon ducts.

The BLIMP Program solves numerically the integral form of the equations describing a laminar, nonsimilar, multi-component, chemically reacting boundary layer. To do this, Kendall and Bartlett, Reference 8, devised a matrix procedure of evaluating the coefficients in the array of equations resulting from a Newton-Raphson method of solution of the boundary-layer equations with given boundary conditions. The general plan of this approach is described below.

The integral boundary-layer equations are written in terms of the primary independent variables: the stream function f, the total enthalpy, H_o, and the elemental mass fraction $\tilde{K}_k$. These

variables are related by a Taylor Series expansion such that f', H_o, and $\tilde{K}_k$ are represented across points in the boundary layer, called nodes, by connected cubic equations. This form of representation is commonly called a spline fit. The Taylor Series for each variable is truncated at the next higher order derivative from that which would appear in the boundary-layer equations. This truncation term is then expressed in terms of lower order derivatives. For example,

$$f''''_{i+1} = \frac{f'''_{i+1} - f'''_i}{\delta_n} \tag{1}$$

This approach is not a conventional finite difference approach, but an integral approach using spline fits between nodes across the boundary layer. Each of the integral terms is expressed by its truncated Taylor Series.

Introducing the normalizing parameter on the nodal network, a_H, the complete assembly of primary variables is then: f_i, f'_i, f''_i, f'''_i, H_i, H'_i, H''_i, $\tilde{K}_k$, $\tilde{K}'_k$, $\tilde{K}''_k$, a_H. During each iteration corrections to the other variables are expressed in terms of corrections to the primary variables. The equations for the conservation of momentum, energy, and chemical species are reduced to linear equations in terms of the corrections on the primary variables. Assuming the pressure is constant across the boundary layers, the corrections take the form:

$$\Delta(\Psi)_i = \text{fn.}\ (\Delta\tilde{K}_k,\ \Delta h_i) \tag{2}$$

The actual solution procedure revolves around the matrix method developed by Aerotherm. The coefficients of the recurrence formulas for the Taylor Series expansions, the linear boundary conditions, a_H constraint, the nonlinear edge boundary conditions, and the boundary-layer equations calculated for the m^{th} iteration form a non-square matrix $||\ A\ ||$ with the number of rows equal to the number of equations, excluding nonlinear surface boundary conditions, and with the number of columns equal to the number of correction variables. The errors can be depicted then as:

$$||\ A\ ||_{I \times J}\ ||\ DV\ ||_J = -\ ||\ E\ ||_I \tag{3}$$

where DV_J is the correction of the J^{th} primary variable.

The matrices are then separated into linear and nonlinear terms by judicious choices

$$\left\| \begin{array}{cc} AL & BL \\ \hline ANL & BNL \end{array} \right\| \left\| \begin{array}{c} VL \\ VNL \end{array} \right\| = - \left\| \begin{array}{c} EL \\ ENL \end{array} \right\| \tag{4}$$

where the AL and BL are square, sparse, arrays, that is most of the elements are zero. After some manipulation one can express the corrections by:

$$|| \, DVL_p \, ||_I = - \, || \, AL_{pp} \, ||_{I \times I}^{-1} \, || \, BL_{pp} \, ||_{I \times J} \, || \, DVNL_p \, ||_J$$

$$+ \, || \, AL_{pp} \, ||_{I \times I}^{-1} \, || \, -EL_p \, ||_I \tag{5}$$

and

$$|| \, DVNL_a \, ||_I = - \, || \, \overline{BNL}_a \, ||_{I \times I}^{-1} \, || \, \overline{BNL}_a \, ||_{I \times J} \, || \, DVNL_b \, ||_J$$

$$+ \, || \, \overline{BNL}_a \, ||_{I \times I}^{-1} \, || \, \overline{ENL} \, ||_I \tag{6}$$

where

$$|| \, \overline{BNL} \, ||_{I \times J} \, || \, DVNL \, ||_J = || \, \overline{ENL} \, ||_I$$

with the coefficients

$$\overline{BNL}_{ij} = BNL_{ij} - \sum_{\ell=1}^{m} ANL_{i,\ell+r} \, || \, AL_{pp} \, ||^{-1} \, || \, BL_{pp} \, ||_{\ell, j-r}$$

$$\overline{ENL}_i = ENL_i - \sum_{p} \sum_{\ell=1}^{m} ANL_{i,\ell+r} \, || \, AL_{pp} \, ||^{-1} \, || \, -EL_{pp} \, ||_{\ell}$$

and the $\overline{BNL}$ array is broken into

$$|| \, \overline{BNL}_a \quad \overline{BNL}_b \, ||_{I \times J} \left\| \begin{array}{c} VNL_a \\ VNL_b \end{array} \right\|_J = || \, \overline{ENL} \, ||_I$$

The nonlinear corrections, $DVNL_b$, comprising Df_w, DH_{Tw}, and $D\tilde{K}_{kw}$, are obtained from the nonlinear wall boundary conditions. With these, the $DVNL_a$ may be computed and then the linear corrections DVL. These corrections are then added to the primary variables, and the next iteration commences.

The output of this computational procedure specifies the following parameters: the static pressure, edge velocity, heat flux, wall shear, and the mass flux of total gaseous components which is separated into the char and the pyrolysis gas components. Also obtained are the momentum-transfer coefficient, $\rho u_e c_f/2$, the heat-transfer coefficient, $\rho u_e C_h$, the blowing rate parameter based on the Stanton number, the momentum thickness, displacement thickness, the shape factor, δ^*/θ, the unit Reynolds number, and the following nodal point informations: f, $f' = u/u_e$, f'', f''', the total enthalpy and its derivatives H_o' and H_o'', (the primes indicate differentiations with respect to the wall distance variable, η) the static enthalpy, temperature, density, viscosity, specific heat, thermal conductivity and Prandtl number.

At this point the data represent quasi-steady-state values of the parameters. To obtain the transient behavior, the CMA program has to be used which allows the transient in-depth prediction of wall temperatures. For each set of data obtained with the CMA as a function of time, another BLIMP calculation is performed to give the transient behavior of the boundary-layer parameters listed above.

The basic assumptions of the CMA program are that (a) a maximum of three components are allowed for the ablator - two resins and one reinforcement, (b) the density history follows an Arrhenius type law, (c) the pyrolysis gases are in equilibrium with the char, (d) the pyrolysis gases pass out of the material immediately, (e) coking cannot occur, (f) the cross-sectional area can vary, and (g) the conduction is one dimensional. The program can be run with any one or a combination of three options. These are (a) a specified surface chemistry (i.e., the species concentration at the surface) to define the film coefficient, (b) a specified surface temperature and recession rate, and (c) a specified radiation view factor and flux. The program was used with option (b).

The fundamental equations for the CMA program are:

1. the energy balance equation:

$$\frac{\partial}{\partial t}\,(\rho h A)_y = \frac{\partial}{\partial y}\,\left(kA\,\frac{\partial T}{\partial y}\right)_t + \frac{\partial}{\partial y}\,(\dot{m}_g h_g)_t \qquad (7)$$

2. an equation for the density history. It is of the Arrhenius type, based upon a number of laboratory experiments:

$$\left(\frac{\partial \rho}{\partial t}\right)_y = -\,Be^{-E/RT}\,\rho_o\,\left(\frac{\rho-\rho_r}{\rho_c}\right)^m \qquad (8)$$

3. the constituent relationship expressing the composition of the ablator:

$$\rho = \Gamma\,(\rho_A+\rho_B) + (1-\Gamma)\,\rho_c \qquad (9)$$

The solution is by finite differences. The equations are expressed as finite differences and the material is separated into an arbitrary number of nodes of fixed and specified size. For ease of calculation the coordinate system is fixed to the receding surface. It requires that the equations be transformed to this moving system. As the surface recedes, nodes are then dropped from the back face of the ablator. The transformed energy equation is solved implicitly for temperature, insuring stability of the solution, but the density equation is solved as an explicit function of temperature due to the complexity of the equation.

The method of solution arranges the differenced temperature equations in a matrix form such as:

$$\begin{aligned} B_1T_1 + C_1T_2' &= fn(q) \\ A_2T_1' + B_2T_2' + C_2T_3' &= D_2 \\ A_3T_2' + B_3T_3' + C_3T_4' &= D_3 \\ A_nT_{n-1}' + B_nT_n' &= f_n(T_{res}) \end{aligned} \tag{10}$$

This is convenient since in the first and last node enter only two unknown temperatures and the surface and heat term. The density relation yields values of gas flow rates. These values make it possible to solve the matrix for the fn(q). The surface energy balance is then performed. The form of the balance equation is:

$$q_{diff} + q_{rad\ in} + \dot{m}_c h_c + \dot{m}_g h_g - q_{rad\ out} - (\rho v)_w h_w - q^* - q_{cond} = 0 \tag{11}$$

where

$$(\rho v)_w = \dot{m}_{g_s} + \dot{m}_c - \dot{m}^*$$

The in-depth solution has supplied $\dot{m}_g$ and $q_{cond} = fn(T_w)$. The general form of solution sought is:

$$\dot{m}^*,\ q_{diff},\ q_{rad\ in},\ h_w,\ q^* = fn(\dot{m}_c, T_w) \tag{12}$$

Using a given value of $\dot{m}_g$ and an initial guess of $\dot{m}_c$, the values for the heat flux terms q_{diff}, $q_{rad\ in}$ and q^* as well as the wall temperature and wall enthalpy are obtained from the energy balance equation using the external, i.e. the gas-side, conditions. Then, the relations for the enthalpies, h_c and h_g,

and the heat flux $q_{rad\ out}$ can be formulated. Thereafter Newton's method is used to get successively better values for the mass removal rate $\dot{m}_c$ to have the energy balance equation converge to zero. The in-depth array then is solved again using the newly computed values of T_w. Solutions without the energy balance equation are also possible by specifying the gas removal rate $\dot{m}_g$ and the wall temperature, or by specifying the radiation fluxes.

RESULTS

Laminar Boundary-Layer Tests

Six test runs were carried out at a Mach number of 3, a supply pressure of approximately 21 atmospheres and stagnation temperatures of about 9000°R. The test durations were about eleven to thirteen seconds. The pressure distribution along the ducts remained essentially unchanged for the duration of the tests. There was a small favorable pressure gradient due to an overcompensation of the boundary-layer growth, as shown in Figure 7. The first duct, L1 of Table I, was corrected for the calculated non-ablative surface boundary-layer growth. During this test a pressure pulse was observed at $x > 2$ inches for about 3 seconds as shown in Figure 8. To eliminate this an estimated increase of the correction was made.

The recording of wall surface temperatures was only partly successful, since the "receding" surface thermocouples failed to recede with the surface and showed erratic readings once exposed to the gas flow. The onset of this erratic behavior, however, allowed us to fix the onset of ablation to about 4 to 4-1/2 seconds after the start of the tests. The in-depth temperature measurements were in general successful. These results will be discussed later in comparison to the BLIMP predictions. It was found, however, that the spacing of the thermocouples - a separation of 0.025 inch from each other was the closest that could be made- was too wide to use the data to evaluate the wall heat transfer.

The gas-wetted surfaces of the ducts developed a glossy, waxy appearance presumably attributable to one of the teflon degradation species. This has been generally observed by other investigators, References 10 and 13. A yellow to brownish discoloration indicated that combustion had taken place.

Two of the ducts showed longitudinal almost parallel striations over the entire length of the duct as shown in Figure 9. The cause of the striations is not yet satisfactorily explained. There was no recorded difference in operating conditions between the runs where the striations were produced and the others where the surface remained smooth. However, the striations tie in with conclusions reached during the analysis of the experimental data, as will be discussed later on. Increased ablation is observed downstream and upstream of the pressure orifices as shown in Figures 10 and 11.

Downstream, the increased ablation is plume shaped, Figure 11, and extends about eight diameters of the pressure orifice beyond the orifice. The maximum width is about two diameters. On the upstream side, the additional ablation did not occur on all orifices and was confined to a distance of two or three orifice diameters.

For all tests, no ablation was measured at the duct entrance because of the contact with the water-cooled nozzle. Then ablation increased very rapidly to a maximum at 1-1/2 to 2 inches from the duct entrance. It then decreased, as expected for a laminar boundary layer. But then, an inversion occurred at $x = 3.5$ inches, and a second maximum appeared at $x \sim 4.3$ to 4.5 inches. The "normal" behavior is well predicted, though with varying degrees of accuracy, by the BLIMP-CMA programs, as seen from Figures 12 and 13. There is strong evidence that the observed anomaly in ablation indicates boundary-layer transition. The momentum thickness Reynolds number variation along the duct, as predicted by BLIMP, showed that a value of 450 was reached at the point of inversion, Figure 14, which is sufficiently large for transition to occur. The calculated boundary-layer profiles support this, Figure 15. Prior to the point of inversion, at $x = 0.96$ inch, the normal laminar profile is predicted, but at $x = 2.76$ inches and $x = 3.96$ inches, just ahead and after the inversion, the profiles exhibit inflections and overshoots both indicative of instability that will lead to transition. The predicted transitional behavior found support in the parallel striations that developed in two of the tests, see Figure 9. Other investigators, References 14 and 15, have found parallel striations in the region of laminar instability. Stationary vortices are assumed to cause the preferential ablation. However, at present, no adequate analysis exists that explains under what conditions they will exist.

The first shear stress measurements were made at a location which is now recognized as being the transitional region of the duct. The balance responded very rapidly as shown in Figure 16 and appeared to approach the predicted steady-state value in about 13 seconds. The minimum exhibited at $\tau = 5.8$ seconds was first erroneously attributed to the transients in the ablation process. In a repeat test, carried out to clarify the matter, two balances were installed in the same duct, one in the definitely laminar region, the other in the transitional region. Readings at the latter location repeated the first data, while in the laminar region, the shear stress was found to decrease uniformly from its nonablation value which is expected; it is shown in Figure 17. The final value is about 36 percent of the predicted cold wall shear stress. It agrees with the BLIMP-CMA prediction in trend and within 22 percent in absolute value as seen from Figure 17. It is possible that inadequate knowledge of the material's properties, such as the viscosity of teflon vapor, can account for this discrepancy.

Steady-state conditions appeared not to be achieved during any of these tests. This was also shown by the CMA calculation. The so called "heat storage term"

$$\int \overline{\rho c_p} \left(\frac{\partial T}{\partial t}\right)_z \frac{A dz}{A_s} \tag{13}$$

has still a finite value, Figure 18. This term accounts for the energy used in increasing the material's temperature at station z as function of time. It has to vanish for steady-state ablation. At $\tau \approx 12$ seconds it was still large in comparison to the surface heating rate at this time, that is about 10 BTU/ft^{2}sec as compared to the surface heat transfer of 158 BTU/ft^{2}sec.

The predicted and measured in-depth wall temperatures compare quite well. Due to the particular thermal characteristics of teflon, the thermocouples had to be installed at depths that would be very close to the surface at the termination of the tests, but should by no means become exposed because of the then resulting erratic behavior, mentioned earlier. The thermocouple location had to be known to within 0.002 inch; this was not quite achieved. It is believed that the experimental data were accurate to not better than 10 percent. The overall agreement with prediction is, however, surprisingly good, as seen from Figure 19. The opposite trends of experimental and computed data are believed to be attributable to the technique employed in computing the in-depth temperatures. It requires that the duct surface temperature is specified, and one then computes the temperature distribution through the material starting from a selected in-depth location. This results in the asymptotic behavior. This specification results in the flattening out of the calculated temperature curve at large values of the time. Under actual test conditions, the surface temperature varies initially quite rapidly but still gives a slower rise of the wall temperature than the predicted value. Then, as steady-state ablation is approached, the surface temperature probably varies more like that predicted by the Scala relation (see discussion on p. 3) but the absolute value will be higher as may be inferred from Figure 20 which compares the predicted surface temperatures with those evaluated from the Scala relation using the measured total ablation. In doing this, it was assumed that $\dot{m}$, the ablation rate, was constant after the onset of ablation which is probably not correct since τ_w and, assuming that Reynolds analogy is true, also the wall heat transfer continues to decrease with time as seen from Figure 17. The latter indicates that H_w increases, since H_r remained constant. The agreement of the BLIMP predicted wall temperatures with those obtained from the time-averaged ablation rates, Figure 20, is within 15°F at a level of 1300°F or 1.2 percent.

Turbulent Boundary-Layer Tests

The turbulent boundary-layer tests were carried out at a Mach number of 2.3, supply pressures of 21 and 28 atmospheres, and temperatures of 4300 to 4600°R. The specific aim for this test

series was to measure the heat transfer to the substructure if the heat shield, i.e. the ablative material, had developed cracks prior to re-entry. These results are reported in detail in Reference 7. Here, only the data of interest with respect to the surface ablative behavior of a heat shield will be included.

The overall ablative behavior of the ducts in this test series, duct 1T through 5T was very uniform increasing from zero at the duct entrance to a moderate maximum at $x \simeq 1$ inch and then leveling off to an almost constant value of about 70 percent of the maximum. The total amount of ablation for a given value of wall heat transfer varied linearly with time, allowing the onset of ablation to be deduced. It was determined to be 0.3 seconds. Ablation was very pronounced as evidenced by the duct static pressure variation as a function of time, shown in Figure 21. The pressure variation, starting after the first second of running time, represents a change in flow Mach number from 2.3 to 2.6. Because of this change in conditions testing times were kept within 2.7 to 6.5 seconds. Skin-friction data were obtained both for the 21 and 28 atmosphere runs. The data indicate that steady-state ablation conditions were probably reached within 2 seconds after the start of the test, when τ_w, the wall shear stress, became practically constant at 60 percent of the predicted nonablative surface value. A comparison with theory was not made for these runs, because a turbulent boundary-layer option of the BLIMP-CMA procedures did not exist at the termination of the present studies.

All ducts in the turbulent boundary-layer series exhibited cross-hatched striation patterns as shown in Figure 22. The patterns started immediately at the duct entrance and formed more regularly if a pressure orifice was not located there. Around a pressure orifice the pattern is more pronounced than elsewhere, as seen in Figure 22. There is a change in pattern size along the duct; whether or not this is connected with the existing pressure gradient could not be concluded from the limited number of tests. The transverse darkened region after the first pressure orifice can also not be explained because the five ducts of this series were all differently instrumented and as a consequence the patterns for each test differed from each other. However, it is believed that this darkened transverse region is incidental, as may be concluded by comparing Figure 22 with Figure 23 which shows another duct, tested under the same conditions. The two transverse dark stripes in this photograph are "cracks" machined into the duct to get information on substructure heating rates for cracked re-entry heat shields (Ref. 7). They were located downstream of the dark region of Figure 22.

SUMMARY AND CONCLUSIONS

Supersonic ablation studies with teflon were carried out in the NOL 3 Megawatt Arc Tunnel. The test conditions were chosen so that the boundary layer in the ducts was predicted to be either

all laminar or all turbulent. Experimental data of wall-static pressure, Pitot pressure, surface and in-depth temperatures, and skin friction were obtained. Total ablation was evaluated from the wall recession. The repeatability of test conditions and results was very good with the exception of the so-called surface thermocouples that were inadequately matched to teflon.

The laminar data were compared with the results of two analytical procedures, the BLIMP-CMA. In general, very good agreement was found between experiments and predictions. An observed ablation anomaly in the downstream half of the ducts was analyzed to be due to laminar instability which was probably followed by transition. This occurs at a location where the computed momentum-thickness Reynolds number is 450.

Shear-stress data in the laminar region followed the predicted trend and were about 36 percent of the predicted cold-wall value. In the transition region, the shear stress as function of time exhibits a minimum and then increases again. A final or steady reading has not been reached at the end of the run.

Parallel striations were found in two of the laminar ducts. Cross-hatched striations were produced in all turbulent tests. Pressure orifices and other surface interruptions have a pronounced effect on the striation pattern.

REFERENCES

1. Aerodynamics Department Staff, "The NOL 3 Megawatt Arc Tunnel," NOLTR 66-80, Sep 1966

2. Winkler, E. M., Humphrey, R. L. and Koenig, J. A., "The NOL Four-Ring, Three-Phase AC Arc Heater, Mk IV," to be published as an NOLTR

3. Solomon, J. M., "The Calculation of Laminar Boundary Layers in Equilibrium Dissociated Air by an Extension of the Cohen and Reshotko Method," NOLTR 61-143, Feb 1962

4. Glowacki, W. J., "Fortran IV Program for Calculating the Turbulent Boundary Layer Growth for Contoured Axisymmetric Nozzles Using Air or Nitrogen," to be published as an NOLTR

5. Bruno, J. R. and Risher, D. B., "Balance for Measuring Skin Friction in the Presence of Ablation," NOLTR 68-163, Sep 1968

6. Warren, W. R., "Determination of Air Stagnation Properties in a High Enthalpy Test Facility," Journal of the Aerospace Sciences, 26, 835, 1959

7. Winkler, E. M., Humphrey, R. L., Koenig J. A. and Madden, M. T., "Investigation of Substructure Heating on Cracked Ablative Heat Shields," to be published as NOLTR 69-122

8. Bartlett, E. P. and Kendall, R. M., "Nonsimilar Solution of the Multi-Component Laminar Boundary Layer by an Integral Matrix Method," Aerotherm Report No. 66-7, Part III, Mar 1967

9. Scala, S. M., "A Study of Hypersonic Ablation," Proceedings of the 10th International Astronautical Congress, Springer Verlag Vienna, 1959

10. Kendall, R. M. and Bartlett, E. P., "A Procedure for Calculating the Nonsimilar, Laminar, Chemically Reacting Boundary Layer Over an Ablating Teflon Body with Coupled Quasi-Steady or Transient Wall Boundary Conditions,"Aerotherm Final Report No. 68-32, Apr 1968

11. Siegle, J. C. and Muus, L. T., "Pyrolysis of Polytetrafluoroethylene," Address to the American Chemical Society Meeting, Sep 1956

12. Friedman, H. L., "The Mechanism of Polytetrafluoroethylene Pyrolysis," General Electric, MSVD Technical Information Series R59SD385, Jun 1959

13. Gregory, N., Stuart, J. T. and Walker, W. S., "On the Stability of Three-Dimensional Boundary Layers with Application to the Flow Due to a Rotating Disk," Boundary Layer Effects in Aerodynamics, Philosophical Library, Inc., 1957

14. Knapp, C. F. and Roache, P. J., "A Combined Visual and Hot Wire Anemometer Investigation of Boundary-Layer Transition," AIAA Journal, 6, 29, 1968

TABLE 1

OPERATING CONDITIONS AND INSTRUMENTATION

Duct Number	Mach Number	Supply Pressure (atm)	Supply Temperature (°R)	Test Time (sec)	Instrumentation
1L	3.03	20.3	7700	13	6 static-pressure orifices
2L	3.04	21.4	8800	13	4 surface thermocouples - 6 static-pressure orifices
3L	3.03	22.0	7870	13	4 thermocouple plugs with 3 thermocouples per plug 6 static-pressure orifices
4L	3.06	22.45	6600	13	1 skin-friction balance 6 static pressure orifices 4 thermocouple plugs
5L	3.03	22.0	7560	13	6 static pressure orifices 1 longitudinal and 1 transverse crack, each with one heat gauge
6L	3.05	22.3	6220	12	2 skin-friction balances
1T	~2.3	20.6	4330	2.7	3 static-pressure orifices 1 longitudinal and 1 transverse crack, each with one heat gauge
2T	~2.3	20.6	4680	5.7	1 static-pressure orifice - longitudinal crack with three heat gauges 1 transverse crack with one heat gauge
3T	~2.3	21	4320	4.2	1 static-pressure orifice 2 transverse cracks, each with one heat gauge
3AT	~2.3	21	4320	6.4	2 static-pressure orifices 2 transverse cracks, each with one heat gauge 1 skin-friction balance
4T	~2.3	28.5	4330	4.4	2 static-pressure orifices 3 transverse cracks, each with one heat gauge
5T	~2.3	28.5	4330	4.6	3 static-pressure orifices 3 in-depth thermocouples 1 skin-friction balance

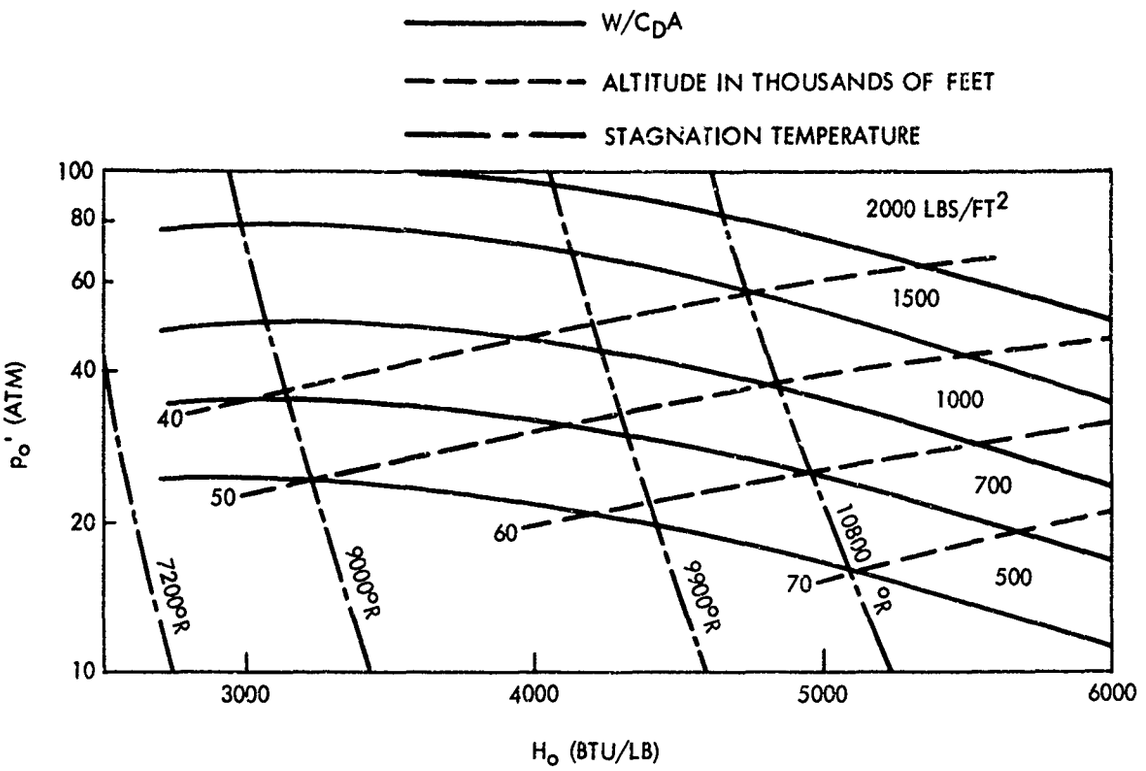

FIG. 1 STAGNATION-POINT PRESSURE VS STAGNATION ENTHALPY FOR A 2500 NAUTICAL MILE MINIMUM ENERGY TRAJECTORY

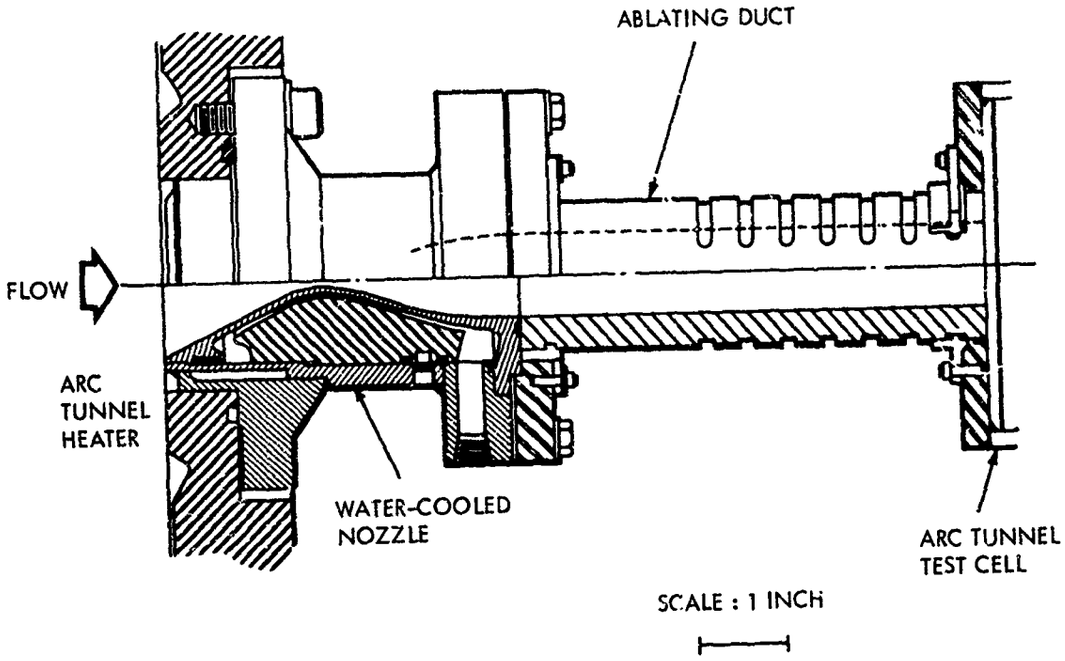

FIG. 2 NOZZLE AND ABLATION DUCT ARRANGEMENT

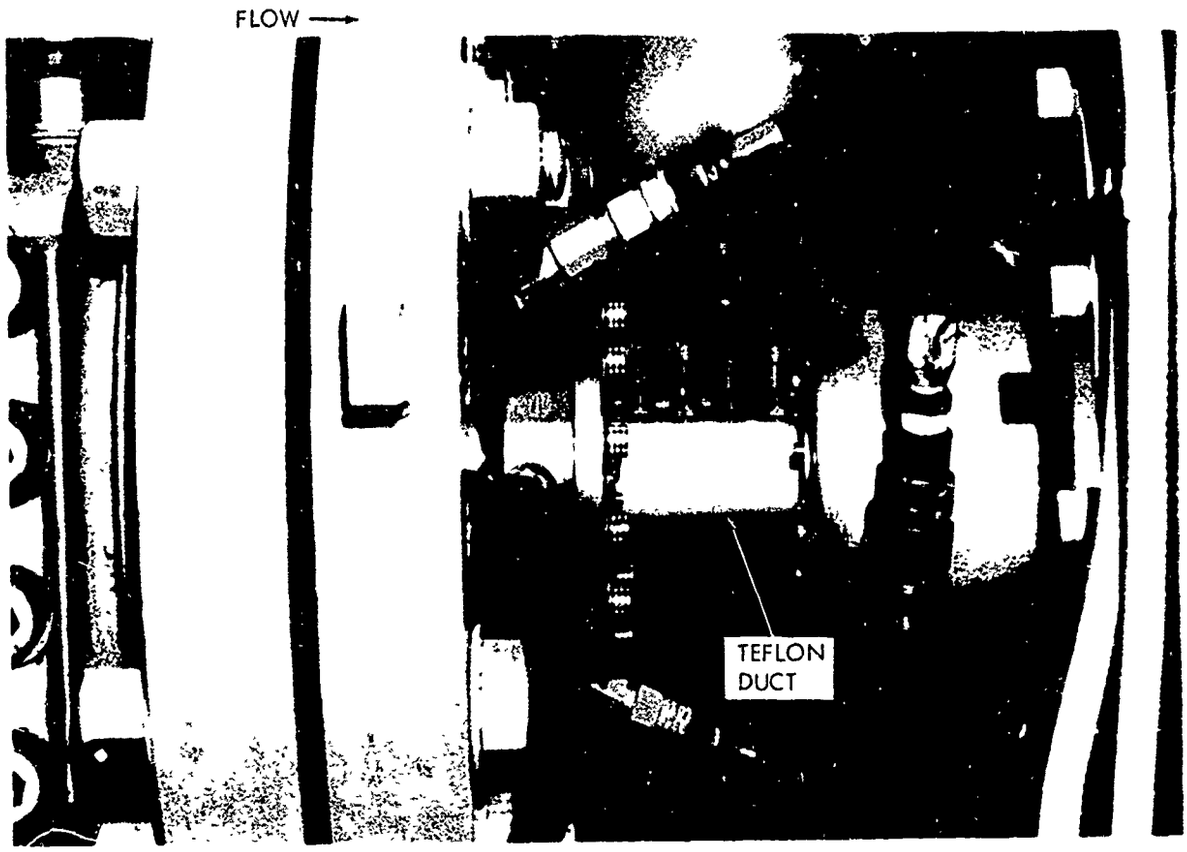

FIG. 3 EXPERIMENTAL SET-UP OF TEFLON DUCT

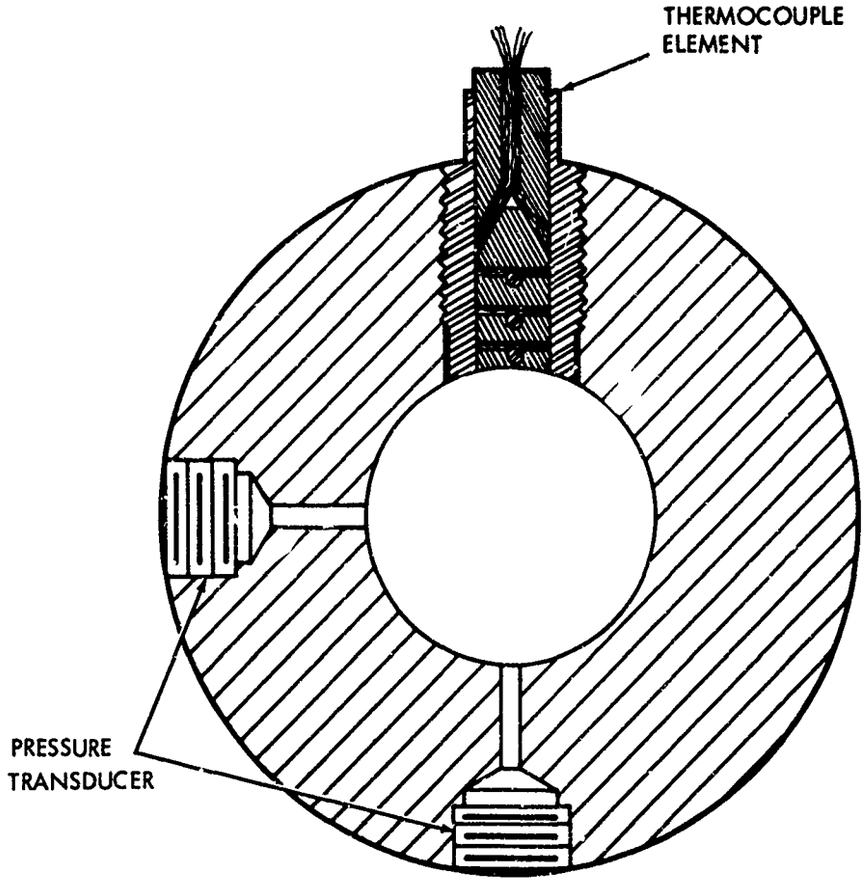

FIG. 4 THERMOCOUPLE PLUG FOR IN-DEPTH TEMPERATURE MEASUREMENT

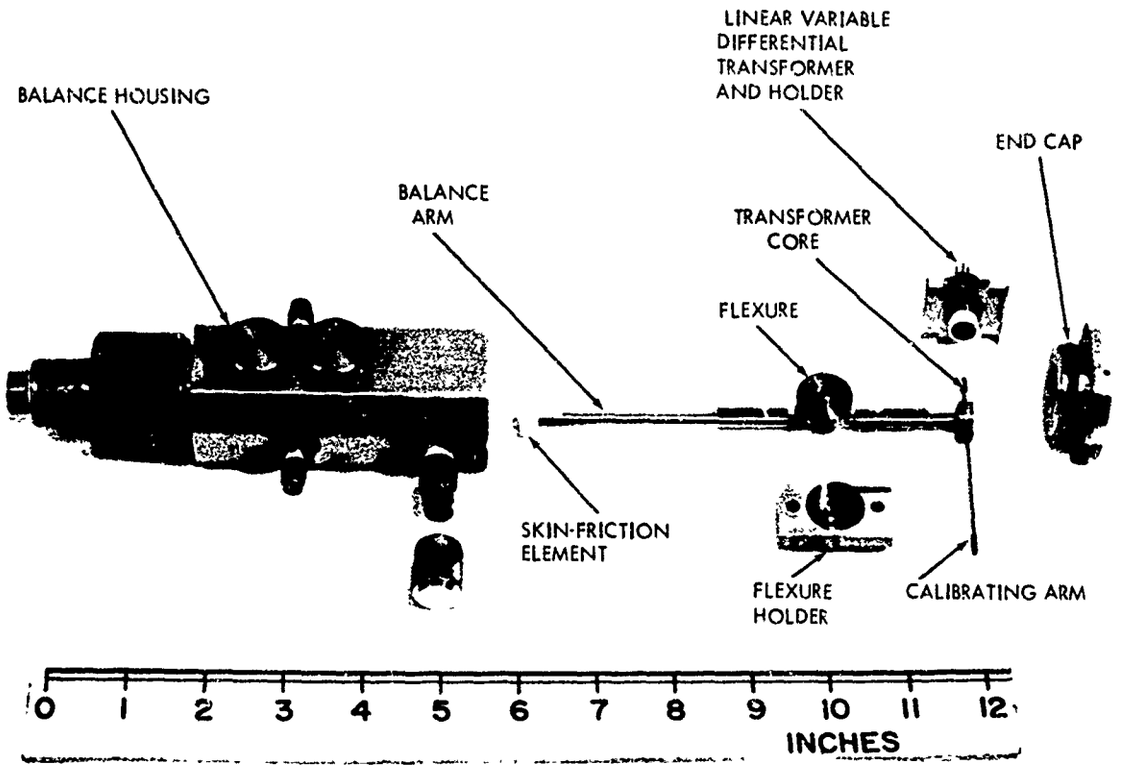

FIG. 5 EXPLODED VIEW OF SKIN FRICTION BALANCE

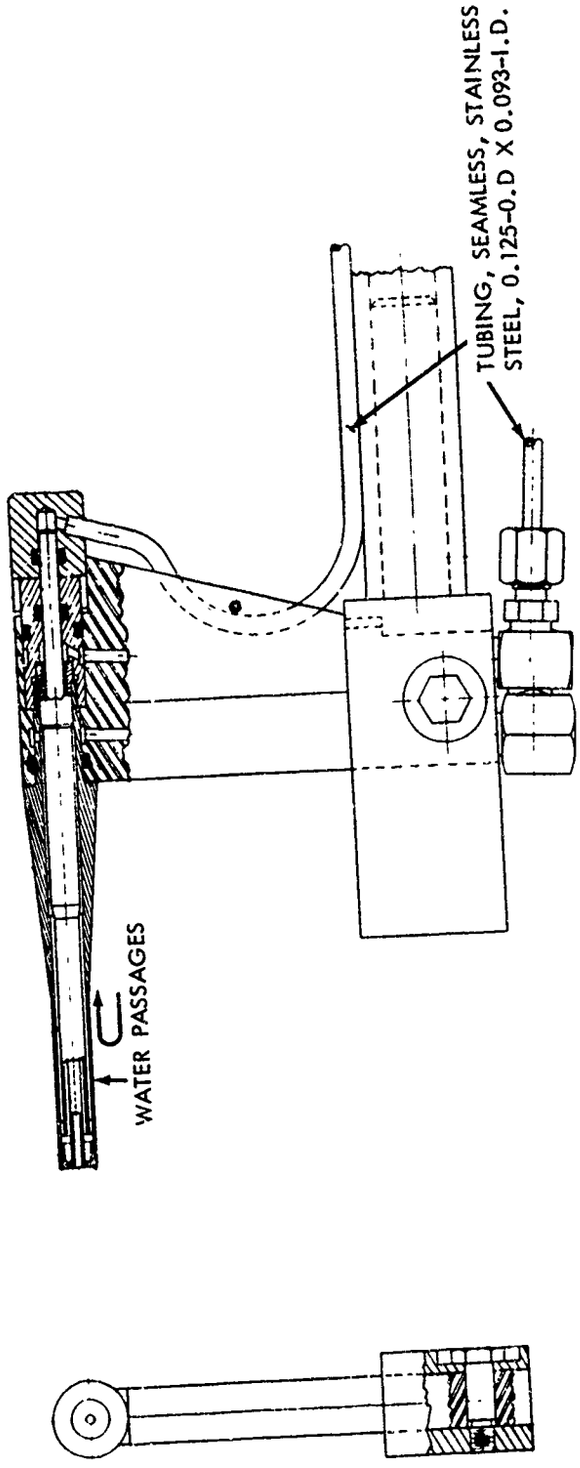

FIG. 6 WATER COOLED PITOT PROBE

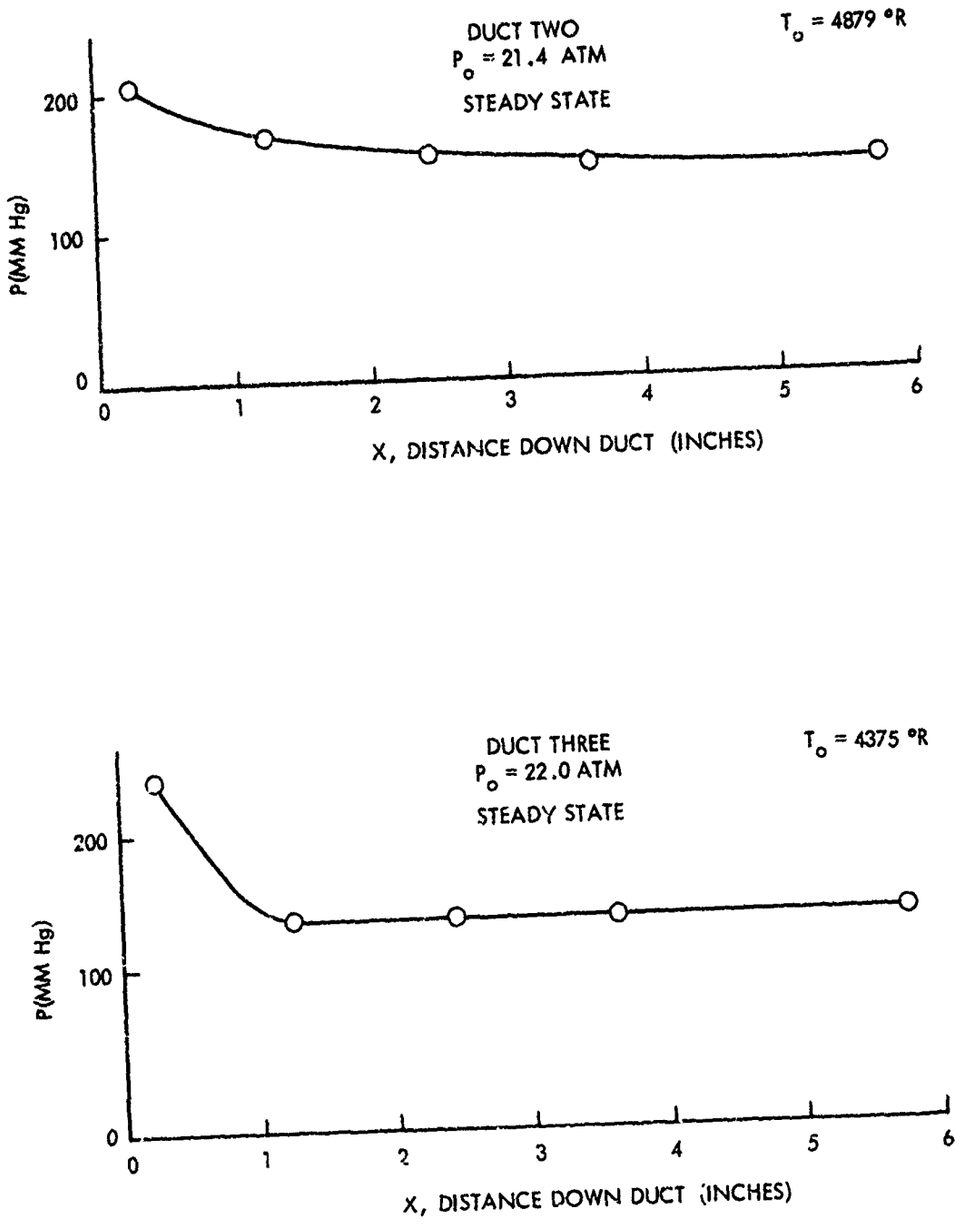

FIG. 7 PRESSURE DISTRIBUTION IN TEFLON DUCT

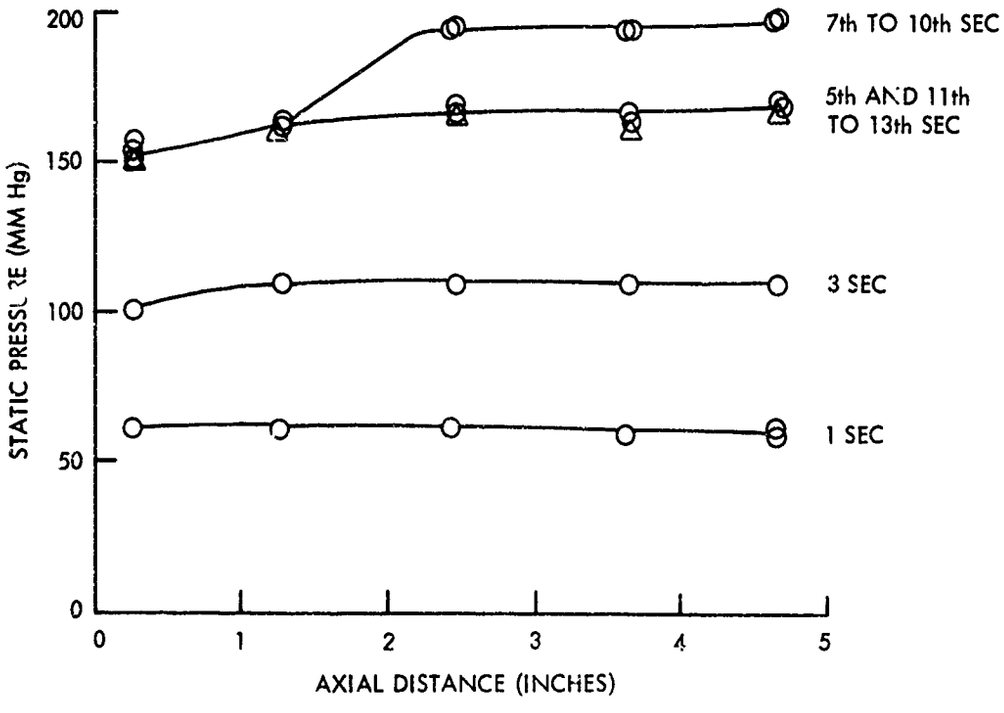

FIG. 8 VARIATION OF PRESSURE DISTRIBUTION IN TEFLON DUCT

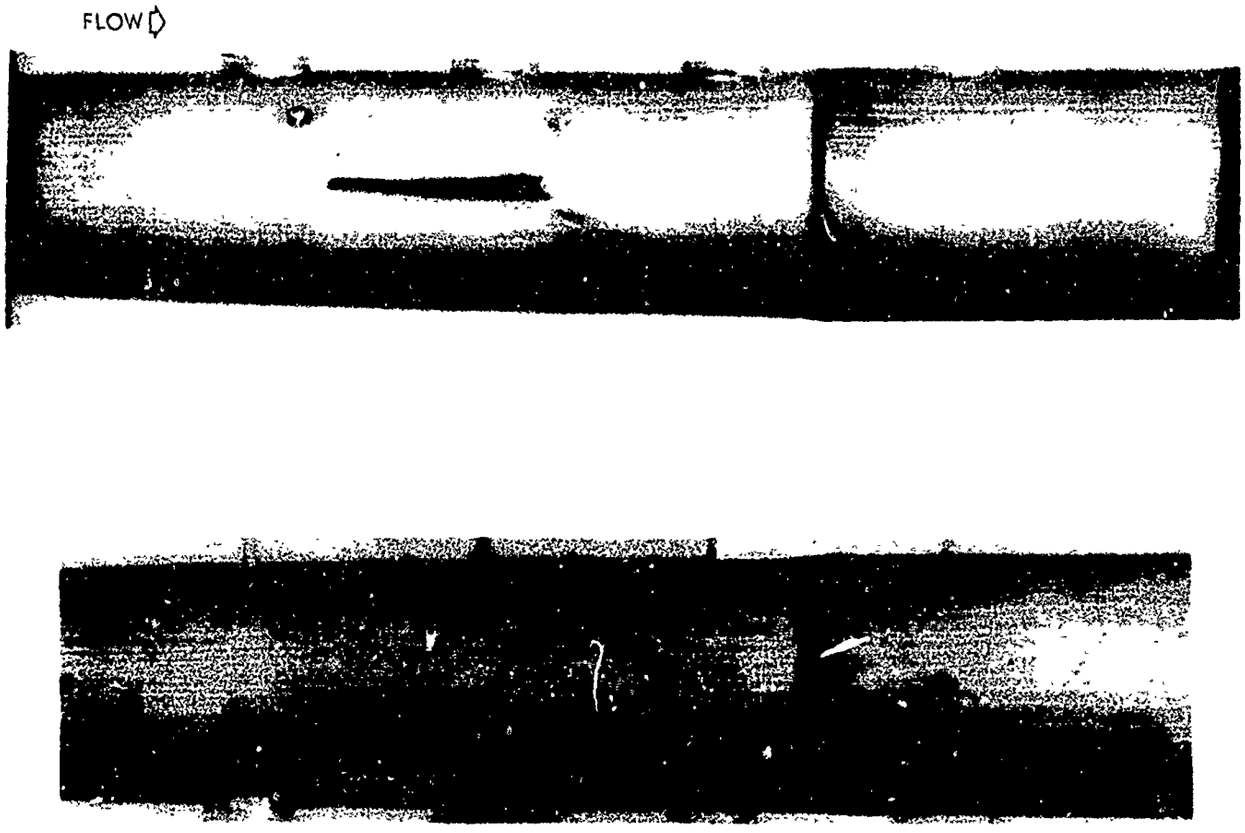

FIG. 9 INSIDE VIEW OF DUCT NUMBER 5L AFTER TEST

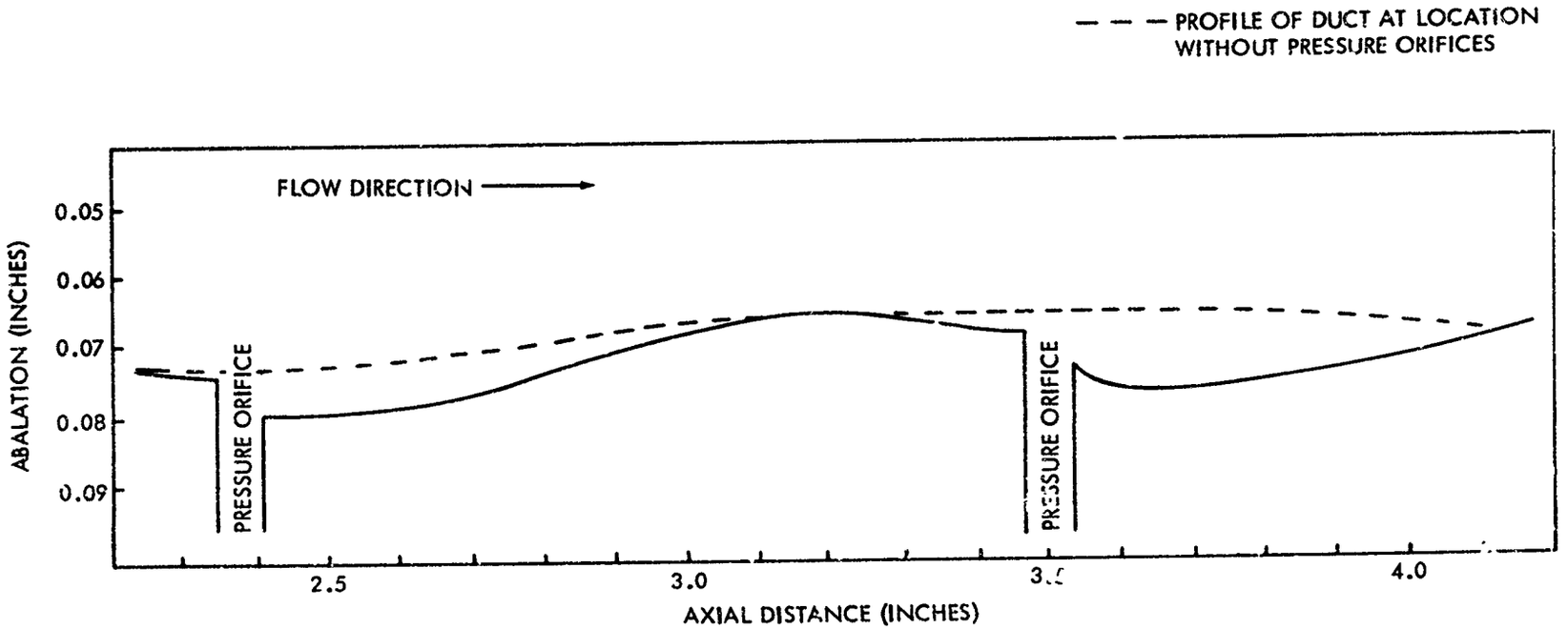

NOLTR 69-125

FIG. 10 ABLATION PROFILE UPSTREAM AND DOWNSTREAM OF PRESSURE ORIFICES

$T_o = 4200^\circ K$, $P_o = 20.4$ atm, $M = 3$, $t = 13$ sec $(d_o/\delta^*)_{av.} = 3$

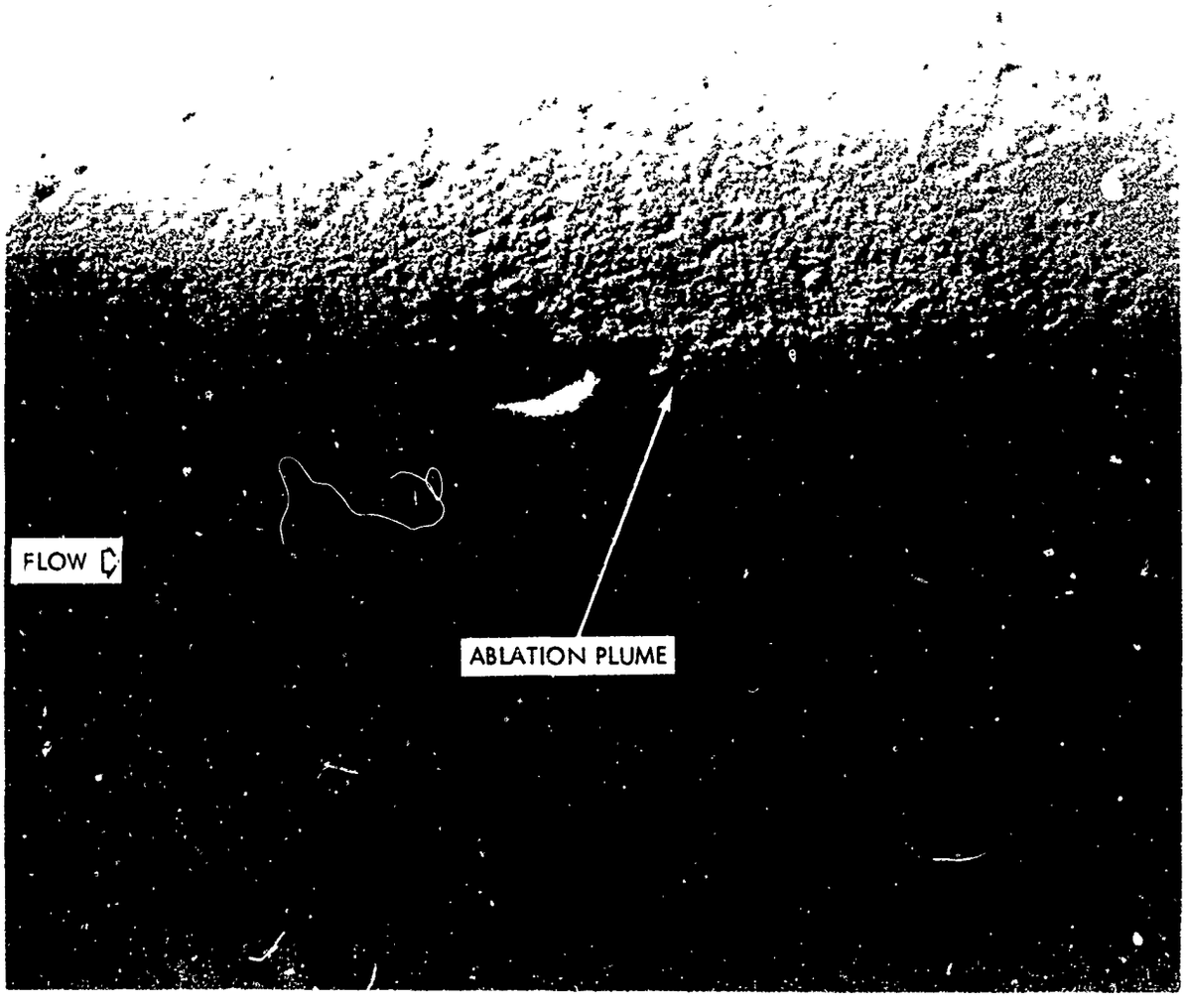

FIG. 11 INCREASED ABLATION DOWNSTREAM OF PRESSURE ORIFICE
(PLASTER MOLD)

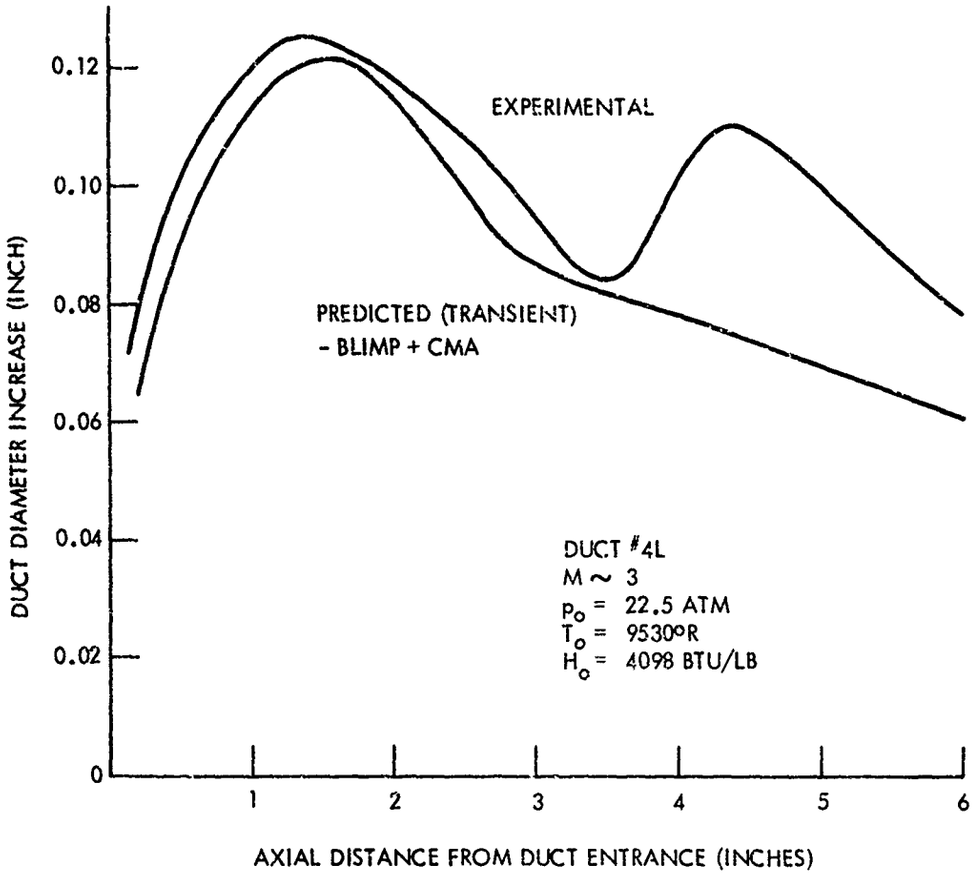

FIG. 12 PREDICTED AND MEASURED TOTAL RECESSION

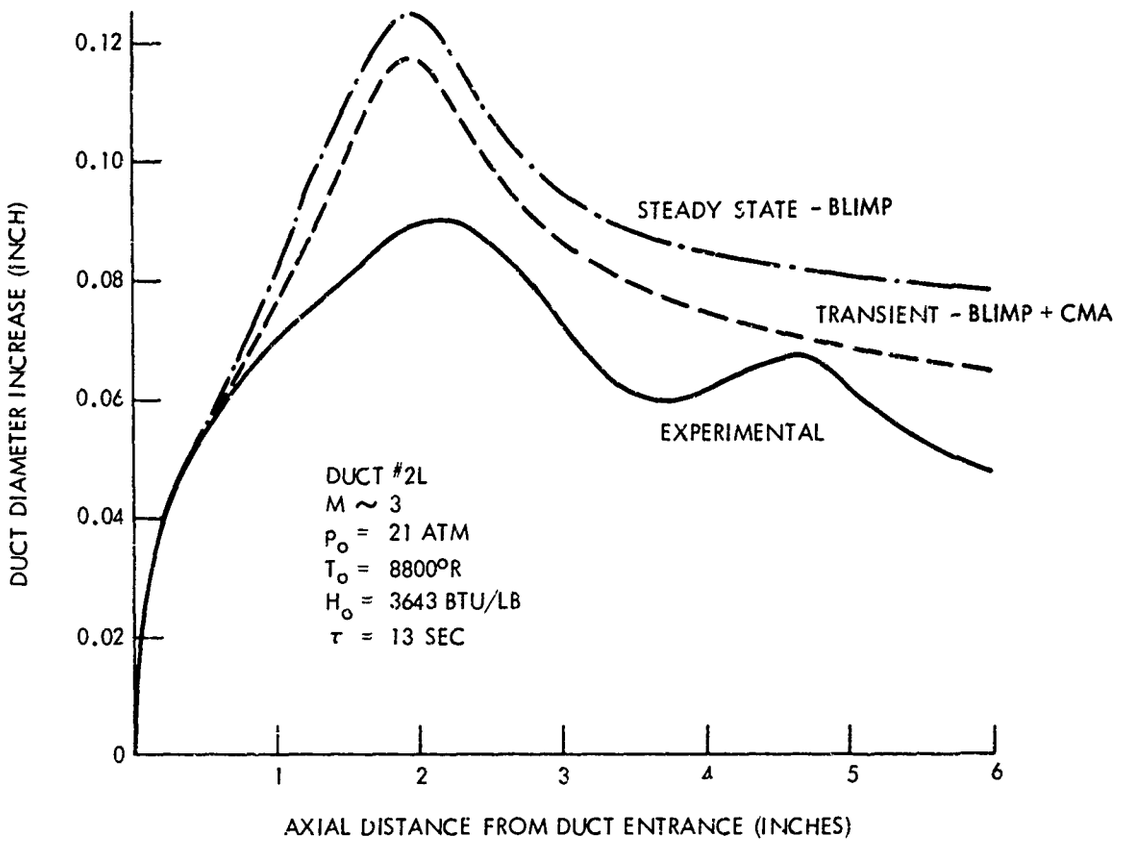

FIG. 13 PREDICTED AND MEASURED TOTAL RECESSION

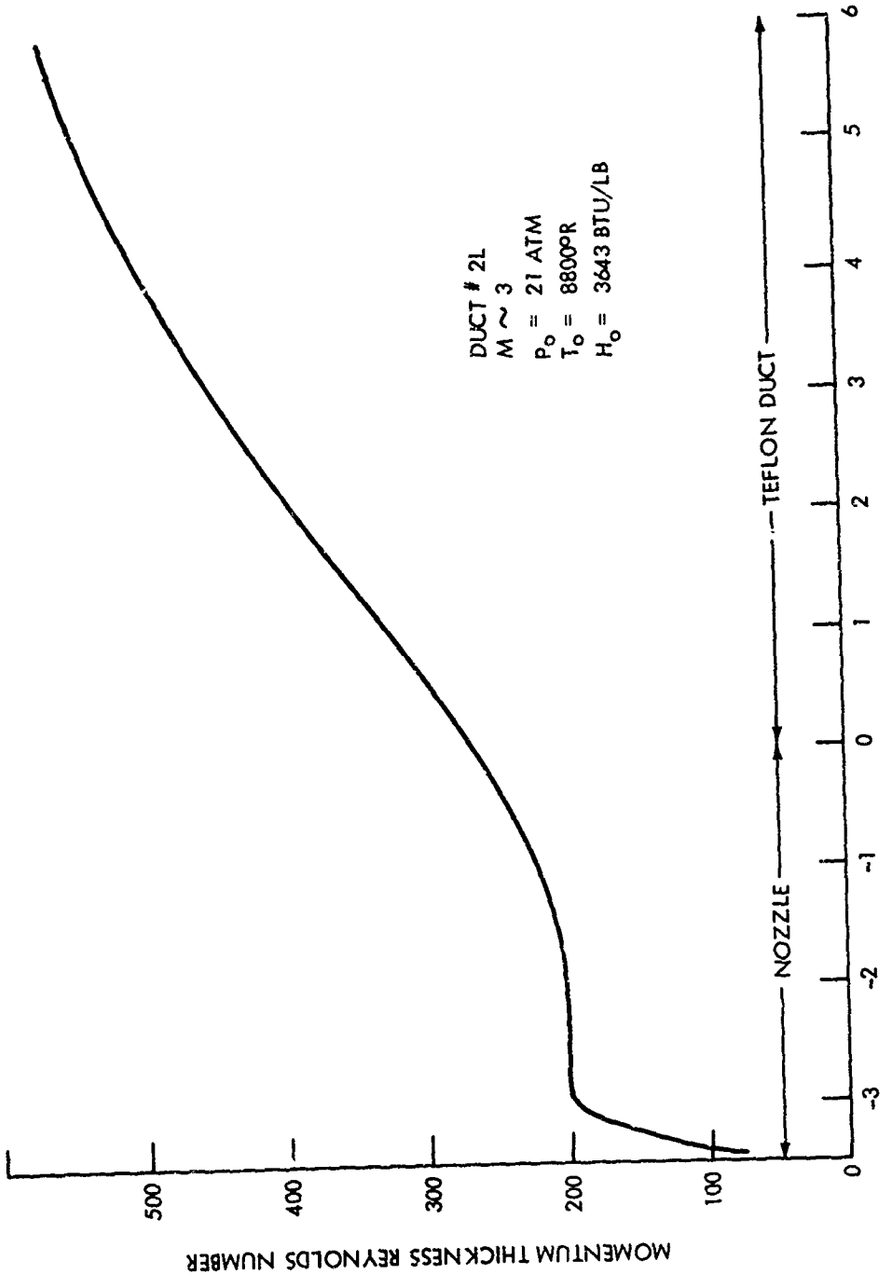

FIG. 14 CALCULATED MOMENTUM THICKNESS REYNOLDS NUMBER VARIATION

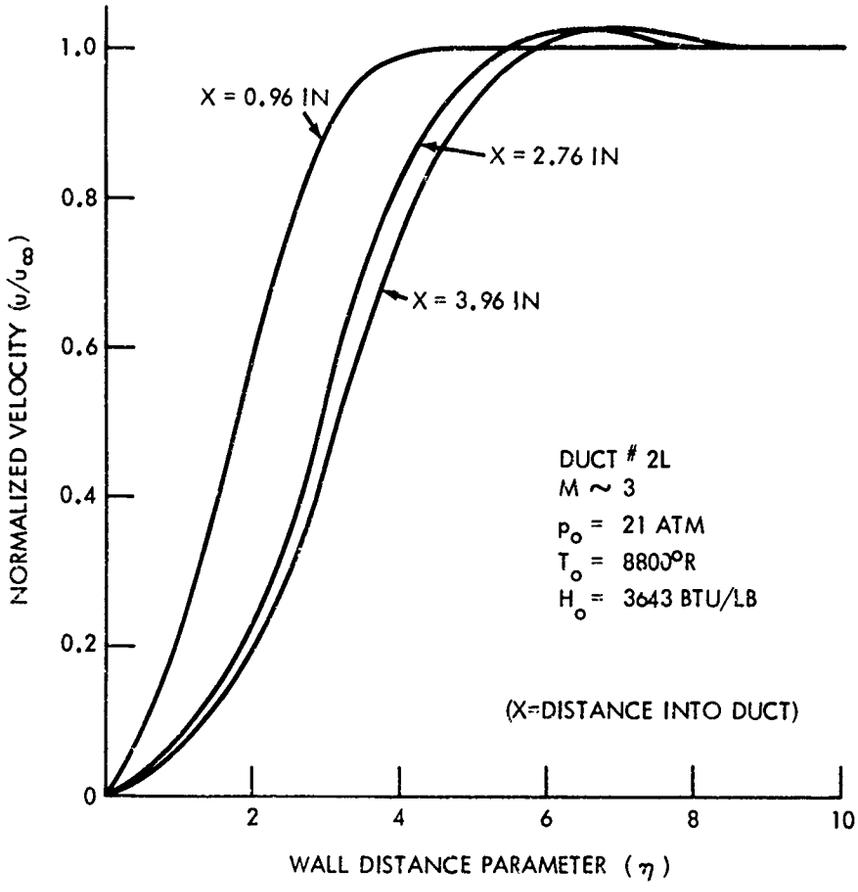

FIG. 15 CALCULATED VELOCITY PROFILES

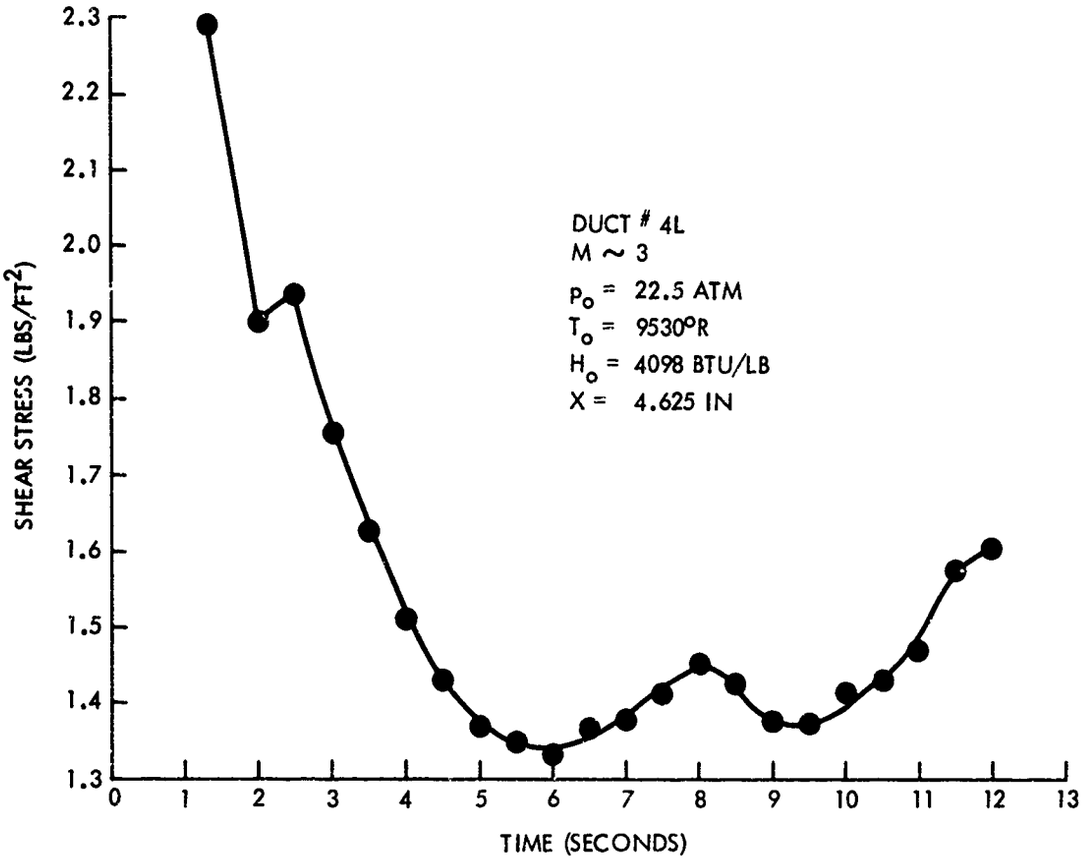

FIG. 16 SHEAR STRESS VARIATION WITH TIME

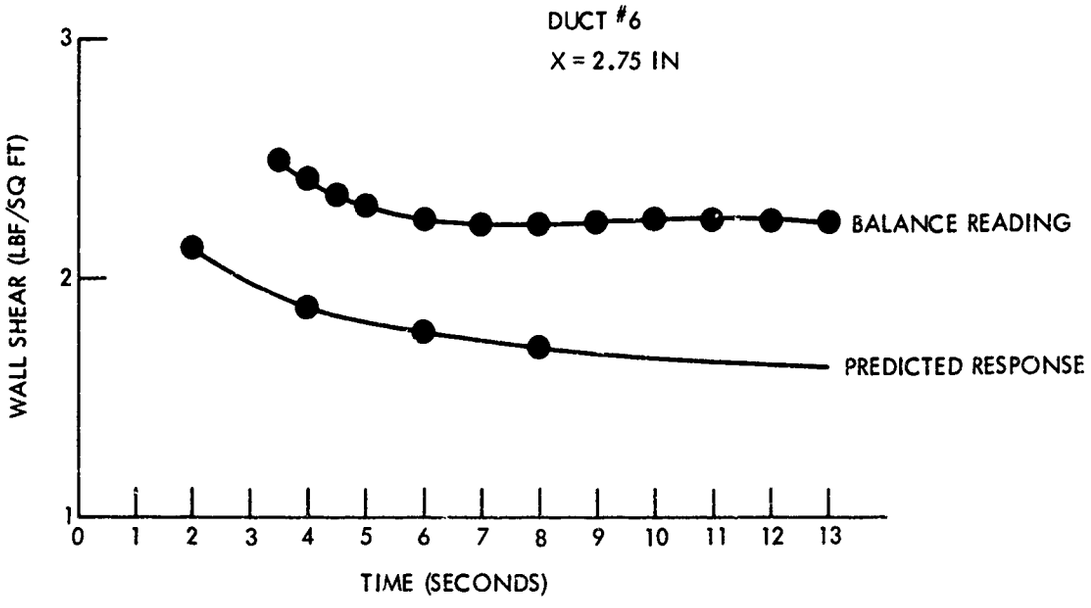

FIG. 17 WALL SHEAR RESPONSE

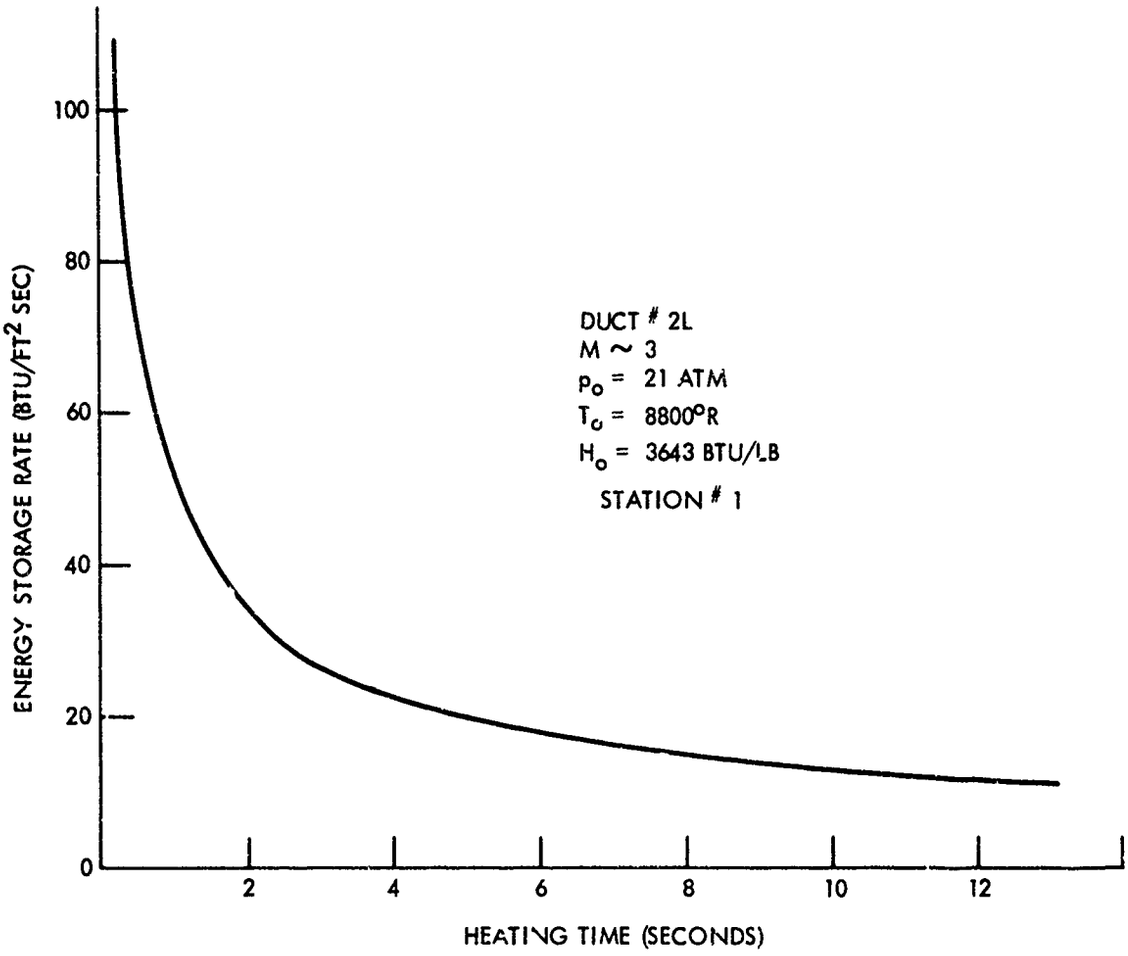

FIG. 18 CMA PREDICTED APPROACH TO STEADY STATE ABLATION

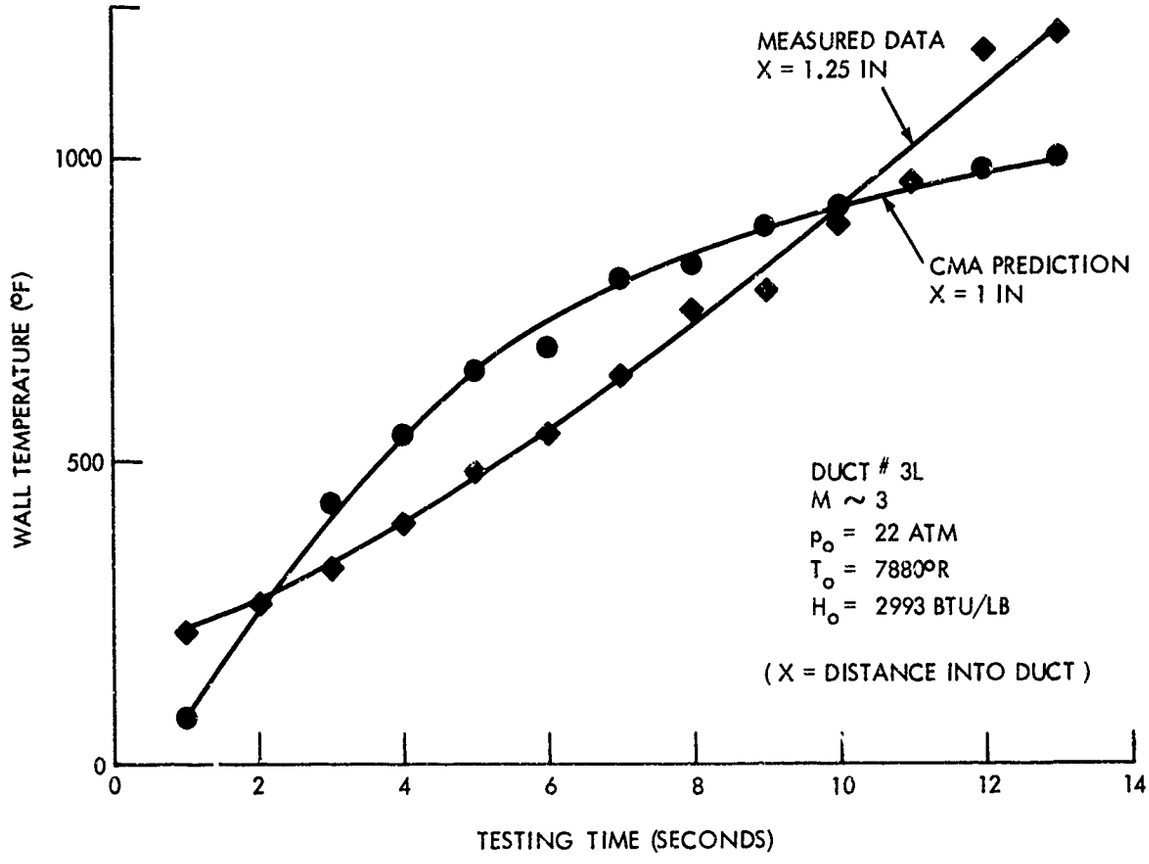

FIG. 19 PREDICTED AND MEASURED IN-DEPTH TEMPERATURES

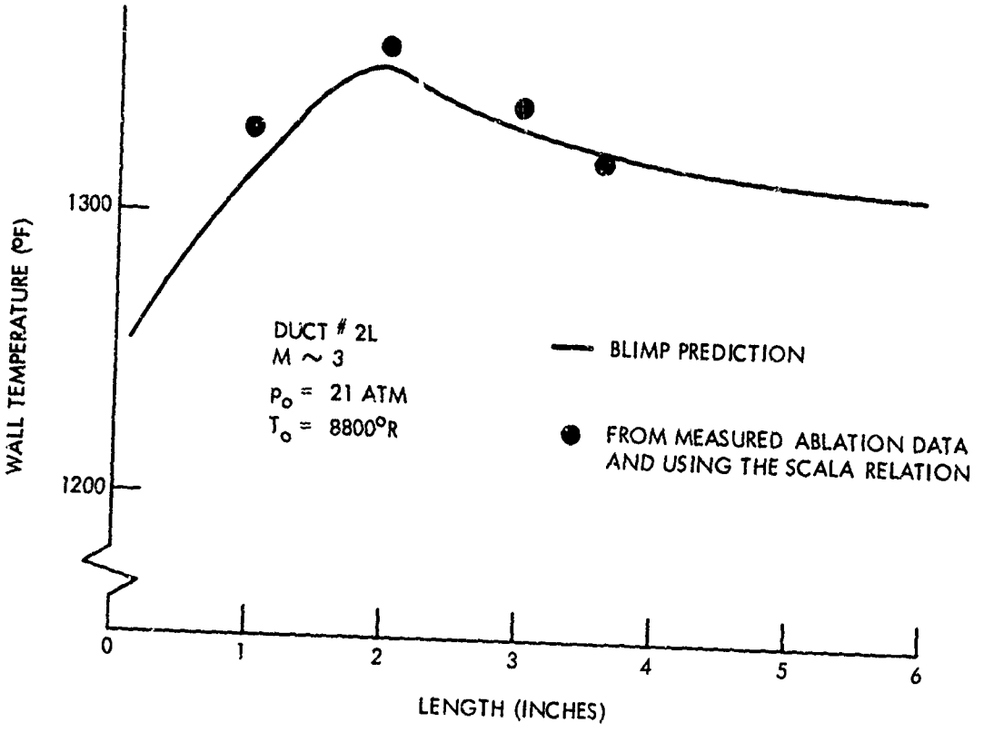

FIG. 20 EXPERIMENTAL AND PREDICTED STEADY-STATE DUCT SURFACE TEMPERATURE

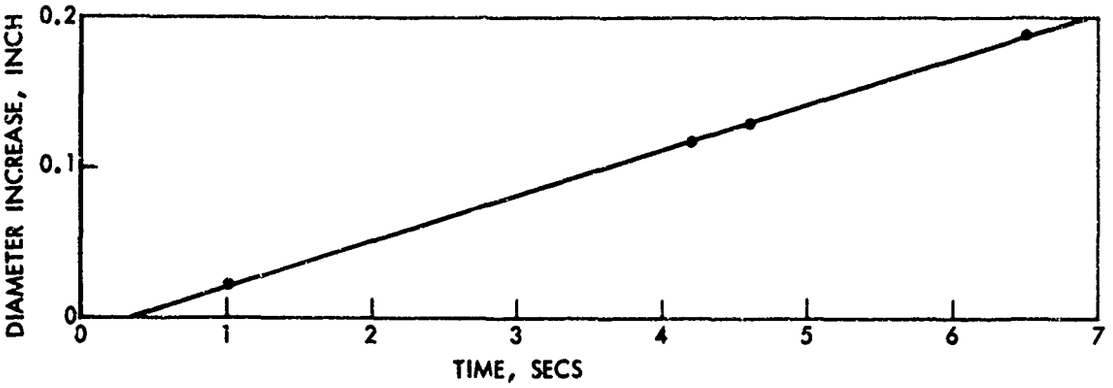

FIG. 21 VARIATION OF TOTAL ABLATION OF FOUR DUCTS AS FUNCTION OF TESTING TIME

FLOW ◊

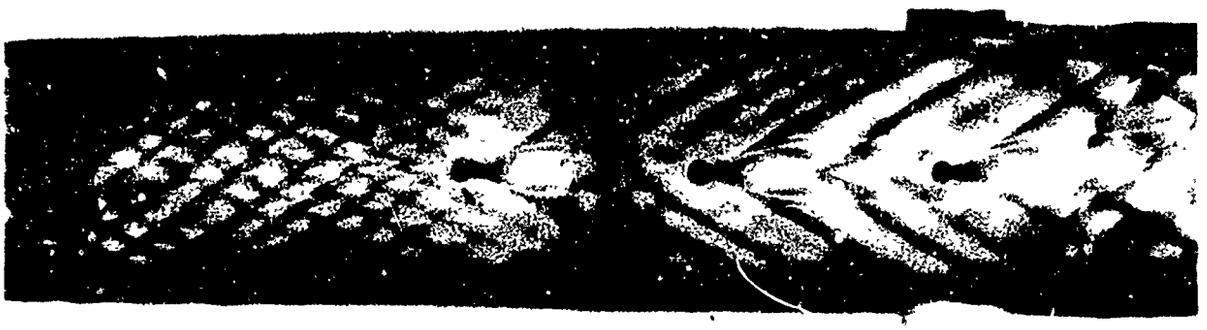

FIG. 22 CROSS-HATCHED STRIATION PATTERN

FLOW ◊

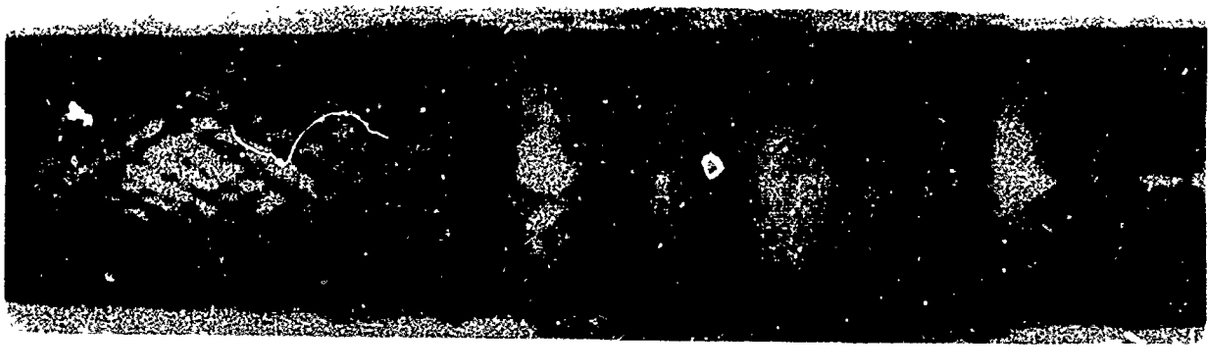

FIG. 23 MODIFICATION OF STRIATION PATTERN DUE TO TRANSVERSE CRACKS

UNCLASSIFIED
Security Classification

DOCUMENT CONTROL DATA - R & D

(Security classification of title, body of abstract and indexing annotation must be entered when the overall report is classified)

1 ORIGINATING ACTIVITY (Corporate author) U. S. Naval Ordnance Laboratory White Oak, Silver Spring, Maryland	2a. REPORT SECURITY CLASSIFICATION UNCLASSIFIED 2b. GROUP

3 REPORT TITLE

Supersonic Ablation Studies with Teflon

4 DESCRIPTIVE NOTES (Type of report and inclusive dates)

final

5 AUTHOR(S) (First name, middle initial, last name)

Eva M. Winkler, Michael T. Madden, Richard L. Humphrey and Joseph A. Koenig

6 REPORT DATE	7a. TOTAL NO OF PAGES	7b. NO OF REFS
6 October 1969	20 plus illus.	14

8a. CONTRACT OR GRANT NO	9a. ORIGINATOR'S REPORT NUMBER(S)
b. PROJECT NO Naval Ordnance Systems Command c. ORDTASK 351-001/029-1/UF 20-322-502 d.	NOLTR 69-125 9b OTHER REPORT NO.S) (Any other numbers that may be assigned this report)

10 DISTRIBUTION STATEMENT

This document has been approved for public release and sale, its distribution is unlimited.

11 SUPPLEMENTARY NOTES	12 SPONSORING MILITARY ACTIVITY
	Naval Ordnance Systems Command Washington, D.C.

13 ABSTRACT

An experimental program has been carried out in the Naval Ordnance Laboratory (NOL) 3 Megawatt Arc Tunnel to study the interaction of ablation and a vehicle's aerodynamic characteristics. The test conditions involved stagnation pressures of 20 to 30 atmospheres, temperatures of 4000 to 9000°R and Mach numbers of 2.3 and 3. The test models, made of teflon, were instrumented for pressure, temperature, heat transfer, and skin-friction measurements. Laminar and turbulent boundary-layer data were obtained. The laminar data were compared with the predictions of a numerical procedure known as BLIMP-CMA. Surprisingly close agreement was found between most of the experimental data and predictions. Ablation-induced transition was observed in all laminar runs. In fully turbulent runs cross-hatched striations were observed. Ablation reduced the wall shear stress by about 60 percent for the laminar runs and by 40 percent for the turbulent runs.

14 KEY WORDS	LINK A		LINK B		LINK C	
	ROLE	WT	ROLE	WT	ROLE	WT
1. Ablation 2. Teflon 3. Ablation-induced transition 4. Cross-hatched striations						